# Design and Preparation of a Novel Temperature-Responsive Ionic Gel. 3. Valence Selective Control of Transport Modes of Ions in Response to Temperature

**Mitsuru Higa* and Tomoko Yamakawa**

*Graduate School of Science and Engineering, Yamaguchi University, Tokiwadai, 2-16-1, Ube City, Yamaguchi 755-8611, Japan*

*Received: December 4, 2007; Revised Manuscript Received: February 21, 2008*

We propose a novel model dialysis system that can valence-selectively control the transport modes of ions in response to temperature change. In a dialysis system consisting of an anionic gel membrane and mixed solutions containing a driving electrolyte and electrolytes with uni-, bi-, and trivalent cations, the dependence of the charge density of the gel and the valence of the ions on the transport modes of the ions through the gel membrane was investigated by computer simulations. The simulations show that the system has four transport types in the transport modes of the cations according to their valence [downhill (transport along their own concentration gradient in the system) and uphill (transport against their own concentration gradient)] in response to the charge density changes: (A) downhill transport of all the cations; (B) uphill transport of trivalent cations, downhill transport of the other cations; (C) uphill transport of bi- and trivalent cations, downhill transport of univalent cations; and (D) uphill transport of all the cations except for the driving cations. To examine the prediction of the simulations, a temperature-responsive anionic gel membrane was prepared from a modified poly(vinyl alcohol) (PVA) containing 2 mol % of sulfonic acid groups and another modified PVA prepared by in situ polymerization of *N*-isopropylacrylamide in a PVA solution. Permeation experiments in a dialysis system consisting of the membrane and mixed electrolyte solutions of NaCl, LiCl, $CaCl_2$, and $LaCl_3$ indicate that the system valence-selectively controls the transport modes of the cations in response to temperature change as predicted in our simulations.

## Introduction

A diffusion dialysis system consisting of a membrane and solutions containing various kinds of ions with different valences will be considered as a simple model of a bioinspired membrane system, such as drug delivery systems. Many researchers have studied stimuli-responsive hydrogels for application in these types of system. Almost all of the hydrogels undergo an abrupt change in volume in response to external stimuli, such as pH,[1–4] temperature,[5–13] electric fields,[14–16] light,[17–19] antigens,[20] and saccharides,[21–25] so that the system can control the permeability of solutes through the membrane in response to these stimuli. These systems would have much higher functionality such as a feedback function when they could control not only the permeability but also the transport modes (downhill and uphill) of specific ions according to their valence in response to external stimuli. In this study, the downhill transport mode refers to the transport of ions along their own concentration gradient in a system and the uphill transport mode refers to the transport of ions against their own concentration gradient. Higa et al.[26,27] have reported that a dialysis system consisting of a temperature-responsive ionic gel and solutions containing univalent cations and bivalent cations modulates the time−concentration profile of the bivalent ions as a sawtooth waveform by controlling the transport modes of just bivalent ions in two ways: downhill and uphill, in response to temperature change. A dialysis system in practical applications in medicine, biotechnology, and industry contain various kinds of ions with different valences such as mixed solutions of adenosine triphosphate, adenosine diphosphate, and adenosine monophosphate. Hence, a dialysis system which can valence-selectively control the transport modes between the ions would be very useful for these applications.

Quantitative studies on the uphill transport of ions through an ion-exchange membrane were first started by Teorell.[28,29] Teorell presented a general equation for the relationship between the ionic composition of the bulk phases and the total membrane potential in the stationary state,[30] where the pH difference between the bulk phases I and II was kept constant. Schwahn and Woermann[31] studied the selective transport of two ionic species of different valency against their concentration gradients. However, their theory is built on the assumption of the stationary state and does not take into account the important role of membrane charge density in uphill transport. Higa and Kira[32] have reported a theoretical simulation method formulated on the basis of both the Donnan equilibrium and the Nernst−Planck equation of flux, which enables the simulation of the uphill transport of ions in a nonstationary dialysis system by numerical computation in a dialysis system consisting of an ionic gel membrane and mixed electrolyte solutions.

This study aims to analyze ionic transport in a model dialysis system consisting of an anionic gel membrane and mixed solutions containing a driving electrolyte and electrolytes with uni-, bi-, and trivalent cations by using computer simulation to investigate the effect of the charge density on the transport modes of ions through the gel membrane. Based on these simulations, we propose a novel dialysis system that can control its valence selectivity by changing the transport modes of ions with different valences according to their valence in response to temperature change. The predictions in the simulations are examined experimentally by the permeation experiment at various temperatures in a dialysis system consisting of a

* To whom correspondence should be addressed. Phone: +81-836-85-9201. Fax: +81-836-85-9203. E-mail: mhiga@yamaguchi-u.ac.jp.

10.1021/jp711437m CCC: $40.75 
Published on Web 05/07/2008

temperature-responsive anionic gel membrane and mixed electrolyte solutions of NaCl, LiCl, $CaCl_2$, and $LaCl_3$.

## Calculations

In the diffusion dialysis system used in this study, an anionic gel membrane lies between two chambers. The two chambers (I and II) contain the $m$ species of $E_k^{(u)}$electrolytes ($1 \le k \le m$) and the $n$ species of $E_j^{(d)}$electrolytes ($1 \le j \le n$). The transport modes of the cations of $E_k^{(u)}$ electrolytes are controlled as uphill or downhill. $E_j^{(d)}$denotes the electrolytes driving the uphill transport. Initially, the concentrations of the transport-controlled electrolytes $E_k^{(u)}$ in chambers I and II are $r_u C_0$ and $C_0$ mol dm$^{-3}$, respectively ($r_u > 1$); hence, the initial concentrations of the electrolytes in chamber I are $r_u$ times higher than those in chamber II. The initial concentrations of the driving electrolytes $E_j^{(d)}$ in chambers I and II are $r_d C_0$ and $C_0$ mol dm$^{-3}$, respectively ($r_d > 1$). Ionic transport in the dialysis systems is calculated under the following assumptions: (a) the surfaces of the membrane are always in a state of the Donnan equilibrium; (b) the boundary effects on the surfaces are negligible; (c) all the electrolytes dissolve perfectly, and ionic activity coefficients are unity both in the aqueous solutions and in the gel membrane; and (d) the standard chemical potentials in the membrane are equal to those in the solutions, respectively.

The Donnan equilibrium and the electroneutrality condition give the following equation:

$$\sum z_i (K_s)^{z_i} C_i^s + z_x C_x = 0 \tag{1}$$

where $z_i$ and $z_x$ are the valence of the $i$th ion and the fixed charge, respectively, and $C_x$ is the membrane charge density; $K_s$ is and the Donnan equilibrium constant[33] at the interface between the membrane and the external solution at the chamber $s$ side

$$(K_s)^{z_i} \equiv \frac{\bar{C}_i^s}{C_i^s} = \exp(-z_i F \Delta\phi_{\mathrm{don}}^s / RT) \tag{2}$$

respectively, where $s$ = I or II; $F$, $T$, and $R$ are the Faraday constant, the absolute temperature, and the gas constant, respectively; and $C_i^s$ and $\bar{C}_i^s$ are the ionic concentrations in the external solution and in the membrane at the chamber $s$ side, respectively. $\Delta\phi_{\mathrm{don}}^s$ is the Donnan potential difference at the interface between the membrane and the external solution at the chamber $s$ side. The Donnan potential difference between the two chambers, $\Delta\phi_{don}$, is given as

$$\Delta\phi_{\mathrm{don}} \equiv \Delta\phi_{\mathrm{don}}^{\mathrm{II}} - \Delta\phi_{\mathrm{don}}^{\mathrm{I}} \tag{3}$$

The flux of the $i$th ion in a gel membrane, $J_i$, is given under the approximation of constant electric field in the membrane as[34]

$$J_i = -\frac{RTz_i\bar{\omega}_i}{d} \ln\beta \frac{\bar{C}_i^{\mathrm{II}} - \bar{C}_i^{\mathrm{I}}\beta^{z_i}}{\beta^{z_i} - 1} \tag{4}$$

where $d$ is the thickness of the membrane; $\beta$ is defined as

$$\beta \equiv \exp(-F\Delta\phi_{\mathrm{diff}}/RT) \tag{5}$$

where $\Delta\phi_{\mathrm{diff}}$ is the diffusion potential difference across the membrane.

The diffusion dialysis system has no electric current

$$I = FS\sum z_i J_i = 0 \tag{6}$$

where $S$ is the membrane area. The combination of eqs 4 and 6 leads to

$$\sum z^2 \frac{X_z - Y_z\beta^z}{\beta^z - 1} = 0 \tag{7}$$

where

$$X_z = \sum_k \bar{\omega}_k^{z+} \bar{C}_k^{z+,\mathrm{II}} + \sum_k \bar{\omega}_k^{z-} \bar{C}_k^{z-,\mathrm{I}} \tag{8}$$

$$Y_z = \sum_k \bar{\omega}_k^{z+} \bar{C}_k^{z+,\mathrm{I}} + \sum_k \bar{\omega}_k^{z-} \bar{C}_k^{z-,\mathrm{II}} \tag{9}$$

and $\bar{\omega}_k^{z+}$ and $\bar{\omega}_k^{z-}$ are the mobilities of $z$-valent cations and anions in the membrane, respectively; $\bar{C}k^{z+,s}$ and $\bar{C}k^{z-,s}$ are the concentrations of $z$-valent cations and anions at the interface the membrane and the external solution at the chamber $s$ side, respectively. $\beta$ is obtained by solving eq 7. The substitution of $\beta$ into eq 4 yields the flux of the $i$th ion.

In a dialysis system consisting of univalent ions, bivalent ions, and trivalent ions, $\beta$ is the solution of the following equation:

$$(\beta+1)(\beta^2+\beta+1)(A_1 - B_1\beta) + 4(\beta^2+\beta+1)(A_2 - B_2\beta^2) + 9(\beta+1)(A_3 - B_3\beta^3) = 0 \tag{10}$$

where

$$\begin{aligned} A_z &= \sum \bar{\omega}_i^{z+} \cdot \bar{C}_i^{z+,\mathrm{II}} + \Sigma\bar{\omega}_i^{z-} \cdot \bar{C}_i^{z-,\mathrm{I}} \\ B_z &= \sum \bar{\omega}_i^{z+} \cdot \bar{C}_i^{z+,\mathrm{I}} + \Sigma\bar{\omega}_i^{z-} \cdot \bar{C}_i^{z-,\mathrm{II}} \end{aligned} \tag{11}$$

and $\Delta\phi_{\mathrm{diff}}$ is obtained in terms of eq 5 as

$$\Delta\phi_{\mathrm{diff}} = -\frac{RT}{F}\ln\beta \tag{12}$$

In an alternative approximation, $J_i$ is given under the assumption of constant concentration gradient in a gel membrane[35] as

$$J_i = -\frac{RT\bar{\omega}_i(\bar{C}_i^{\mathrm{II}} - \bar{C}_i^{\mathrm{I}})}{d}\left[1 - \frac{z_i}{\ln\dfrac{\bar{C}_i^{\mathrm{II}}}{\bar{C}_i^{\mathrm{I}}}} \frac{\displaystyle\sum_i z_i\bar{\omega}_i(\bar{C}_i^{\mathrm{II}} - \bar{C}_i^{\mathrm{I}})}{\displaystyle\sum_i \frac{z_i^2\bar{\omega}_i(\bar{C}_i^{\mathrm{II}} - \bar{C}_i^{\mathrm{I}})}{\ln\dfrac{\bar{C}_i^{\mathrm{II}}}{\bar{C}_i^{\mathrm{I}}}}}\right] \tag{13}$$

and the diffusion potential is also obtained as

$$\Delta\phi_{\mathrm{diff}} = -\frac{RT}{F} \frac{\displaystyle\sum_i z_i\bar{\omega}_i(\bar{C}_i^{\mathrm{II}} - \bar{C}_i^{\mathrm{I}})}{\displaystyle\sum_i \frac{z_i^2\bar{\omega}_i(\bar{C}_i^{\mathrm{II}} - \bar{C}_i^{\mathrm{I}})}{\ln\dfrac{\bar{C}_i^{\mathrm{II}}}{\bar{C}_i^{\mathrm{I}}}}} \tag{14}$$

The total membrane potential difference between the two chambers, $\Delta\phi$, is given as

$$\Delta\phi \equiv \Delta\phi_{\mathrm{don}} + \Delta\phi_{\mathrm{diff}} \tag{15}$$

The normalized electrochemical potential difference of the $i$th ion between the two chambers, $\Delta\mu_i$, is defined as:

$$\Delta\mu_i \equiv \ln\frac{C_i^{\mathrm{II}}}{C_i^{\mathrm{I}}} + \frac{z_i F\Delta\phi}{RT} \tag{16}$$

The time evolutions of the ionic concentrations in the two chambers are given from the following equations:

$$C^{\mathrm{I}}_{i,t_n+1} = C^{\mathrm{I}}_{i,t_n} - J_{i_n} S\Delta t/V^{\mathrm{I}} \quad (17)$$

$$C^{\mathrm{II}}_{i,t_n+1} = C^{\mathrm{II}}_{i,t_n} + J_i S\Delta t/V^{\mathrm{II}} \quad (18)$$

where $C^{\mathrm{I}}_{i,t_n}$ and $C^{\mathrm{II}}_{i,t_n}$ are the ionic concentration at time $t_n$ in chambers I and II, respectively; $\Delta t = t_{n+1} - t_n$; $S$ is the membrane area; and $V^{\mathrm{I}}$ and $V^{\mathrm{II}}$ are the volumes of chambers I and II, respectively.

Although there have been many reports on the measurement of mobility in ionic gels,[36–38] it is difficult to experimentally quantitate the ion mobility in a gel membrane, particularly gel membranes with low water content and high charge density. Mackie and Meares[39] estimated the mobility in a swollen membrane as a function of water content, $H$, of the membrane and the mobility in an aqueous solution, $\omega_i$. Higa et al.[40] reported that the experiments of the diffusion coefficient of 1−1 type electrolytes such as KCl in swollen poly(vinyl alcohol) (PVA) gel membranes almost agree with the prediction of the Mackie and Meares theory, but those of electrolytes having multivalent ions such as $CaCl_2$ have smaller values than the prediction. Higa et al. estimated the mobility of the $i$th ion in the membrane $\bar{\omega}_i$, from permeation experiments through PVA membranes, as

$$\bar{\omega}_i = \frac{a(H)^3}{(2-H)^2}\omega_i \quad (19)$$

where $a$ is the correction factor for the Mackie and Meares theory. The values of the mobility in an aqueous solution, $\omega_i$, for $Na^+$, $Li^+$, $Ca^{2+}$, $La^{3+}$, and $Cl^-$ ions are $5.4 \times 10^{-13}$ mol m$^2$ J$^{-1}$ s$^{-1}$, $4.2 \times 10^{-13}$ mol m$^2$ J$^{-1}$ s$^{-1}$, $3.2 \times 10^{-13}$ mol m$^2$ J$^{-1}$ s$^{-1}$, $2.5 \times 10^{-13}$ mol m$^2$ J$^{-1}$ s$^{-1}$, and $8.2 \times 10^{-13}$ mol m$^2$ J$^{-1}$ s$^{-1}$, respectively.[41]

## Experimental Section

**Synthesis of Graft Polymer.** A temperature-responsive polymer was prepared by in situ polymerization of *N*-isopropylacrylamide in a PVA solution as follows: PVA [Aldrich] (1.0 g), NIPAAm [Wako Pure Chemical Industries, Ltd.] (11.0 g), and potassium persulfate (0.06 g) as an initiator were dissolved in 80 mL of dimethyl sulfoxide (DMSO). The glass tube containing the solution was sealed by conventional methods and immersed in an oil bath held at 40 °C for 20 h. The reactant was poured into acetone to precipitate the T-responsive polymer.

**Preparation of Gel Membrane.** The T-responsive polymer obtained (1.50 g), a polyanion [poly(vinyl alcohol-*co*-2-acrylamido-2-methylpropane sulfonic acid)] (Kuraray Co. Ltd.) (0.32 g), and PVA (0.76 g) were dissolved in 34 mL of DMSO. After casting the solution on an acrylic plastic plate and drying it at 50 °C on a hot stage (NISSIN, NHP-45N), a freestanding membrane (its thickness is 0.1 mm) was obtained. The resulting membrane was cross-linked physically by annealing the membrane at 160 °C for 20 min in an electric drying oven (ADVANTEC, FS-320). After, this membrane was cross-linked chemically in an aqueous solution of a mixture of 0.025 vol % glutaraldehyde, 0.1 mol dm$^{-3}$ HCl, and 2 mol dm$^{-3}$ NaCl at 25 °C for 24 h.[42]

**Measurement of Water Content.** The water content in the *T*-responsive gel membrane was determined by the same methods as described elsewhere.[42] The membrane, weighted in the dry state, was immersed in deionized water at various temperatures for 3 days and was weighted in the wet state. The water content, $H$, is derived from weights in the wet state, $W_w$, and in the dry state, $W_d$, as

$$H \equiv \frac{[(W_w - W_d)/1.0]}{[(W_w - W_d)/1.0] + [W_d/1.3]} \quad (20)$$

where 1.0 and 1.3 are the densities of water and PVA, respectively.

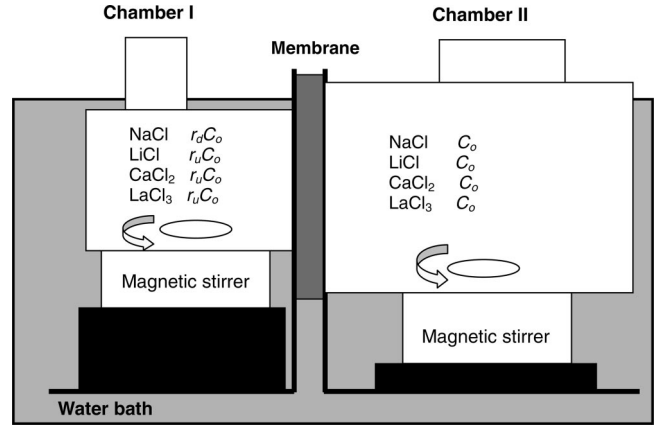


**Figure 1.** Schematic diagram of the permeation experiment, where $C_0$ is the initial concentration of the electrolytes at chamber II; $r_d$ is the initial concentration ratio of the driving electrolyte between the two chambers; and $r_u$ is the initial concentration ratio of the transport-controlled electrolytes between the two chambers.

**Measurement of Membrane Thickness.** The membrane was immersed in deionized water at various temperatures for 3 days. The membrane was removed from the water, and its thickness in the wet state was measured using a thickness gauge (TECLOCK SM-114).

**Determination of the Charge Density.** The charge density was estimated from membrane potential data. The potential was measured at various temperatures by using an acrylic plastic cell of two parts separated by the *T*-responsive gel membrane. One chamber of the cell was filled with KCl solutions of various concentrations (0.01, 0.03, and 0.1 mol dm$^{-3}$), $C_0$. The other chamber was filled with KCl solutions whose concentration was 5 times higher than those in the first chamber ($r = 5$). From the measured membrane potentials, $\Delta\phi$, the charge density, $C_x$, was calculated in terms of[28,43]

$$\Delta\phi = -\frac{RT}{F}\ln\left(r\frac{\sqrt{C_x^2 + (2C_0)^2} - C_x}{\sqrt{C_x^2 + (2rC_0)^2} - C_x}\right) - \frac{RT}{F}W\ln\left(\frac{\sqrt{C_x^2 + (2rC_0)^2} - C_xW}{\sqrt{C_x^2 + (2C_0)^2} - C_xW}\right) \quad (21)$$

where $W = (\bar{\omega}_K - \bar{\omega}_{Cl})/(\bar{\omega}_K + \bar{\omega}_{Cl})$ and $\bar{\omega}_K$ and $\bar{\omega}_{Cl}$ are the $K^+$ and $Cl^-$ mobilities in a gel membrane, respectively. Parameters $W$ and $C_x$ were adjusted so that the left-hand side of eq 21 fits the experimental data of $\Delta\phi$ at various KCl concentrations.

**Permeation Experiments.** Permeation experiments at the desired temperatures (10, 32, and 50 °C) were performed by using an acrylic plastic cell of two parts separated by the T-responsive gel membrane, as shown in Figure 1. In this system, the transport-controlled electrolytes were LiCl, $CaCl_2$, and $LaCl_3$, and the driving electrolyte was NaCl. The initial concentration of the transport-controlled electrolytes and the driving electrolyte at chamber II, $C_0$, was $5.0 \times 10^{-4}$ mol dm$^{-3}$; the initial concentration ratio of the driving electrolyte between

the two chambers, $r_d$, was 300; and the initial concentration ratio of the transport-controlled electrolytes between the two chambers, $r_u$, was 4. Hence, initially, the concentration of the transport-controlled cations at chamber I were 4 times higher than that at chamber I, and the concentration of the driving electrolyte at chamber I was 300 times higher than that at chamber II. The volumes of chambers I and II were 100 $cm^3$ and 400 $cm^3$, respectively. The effective membrane area of the cell was 7.07 $cm^2$. A volume of 0.75 mL of the solution in chamber I was sampled at appropriate time intervals to measure the concentration of $Li^+$ ions using a flame photometer (Hitachi Co, Z-5310), the concentration of $Ca^{2+}$ ions using an ion chromatograph (Hitachi Co. L-3710), and the concentration of $La^{3+}$ ions using an atomic absorption spectrometer (Hitachi Co, Z-5310).

## Results and Discussion

**Simulation.** The time evolution of the concentration and electrochemical potential differences of the transport-controlled cations and membrane potentials in a model dialysis system were simulated. The system consists of a model gel membrane and two chambers which contain LiCl, $CaCl_2$, and $LaCl_3$ as transport-controlled electrolytes, and NaCl as the driving electrolyte. For the conditions in the simulations, the initial concentrations and volume of the two chambers and the effective membrane area were all set to be the same as those of the permeation experiments. The water content and thickness of the gel membrane were set as 0.50 and 100 $\mu$m, respectively, and the temperature in the system was set as 25 °C. The ionic mobility of all of the ions was calculated in terms of eq 19, setting $a = 1$ in each case. The calculated values of the mobility of $Na^+$, $Li^+$, $Ca^{2+}$, $La^{3+}$, and $Cl^-$ ions in the gel membrane under the conditions are $3.0 \times 10^{-14}$ mol $m^2$ $J^{-1}$ $s^{-1}$, $2.3 \times 10^{-14}$ mol $m^2$ $J^{-1}$ $s^{-1}$, $1.8 \times 10^{-14}$ mol $m^2$ $J^{-1}$ $s^{-1}$, $1.4 \times 10^{-14}$ mol $m^2$ $J^{-1}$ $s^{-1}$, and $4.6 \times 10^{-14}$ mol $m^2$ $J^{-1}$ $s^{-1}$, respectively. In our systems, the membrane potential differences have positive values if the potentials in chamber II are higher than those in chamber I, and the electrochemical potential differences have positive values if the electrochemical potentials in chamber II are higher than those in chamber I.

***A. Time Evolution of the Concentration and Electrochemical Potential of the Cations and Membrane Potentials through an Anionic Membrane with Various Charge Densities.*** Figure 2 shows simulations of the evolution of ionic transport in the system when the charge density of the gel membrane is 0.035 mol $dm^{-3}$. Part a of Figure 2 shows that the concentrations of the transport-controlled cations in chamber I decrease with permeation time, $t$. The initial concentrations of the cations in chamber I are $r_u$ (=4) times higher than those in chamber II. This means that the downhill transport of the three cations occurs. In our system, this transport situation (downhill transport of the three cations) is defined as type A transport. Part b of Figure 2 shows that, initially, $\Delta\phi_{don}$ is 25 mV, a value which decreases with time, while the initial value of $\Delta\phi_{diff}$ is −15 mV, and this increases with time. The reason why $\Delta\phi_{diff} < 0$ is because the mobility of the cations of the driving electrolyte, $Na^+$ ions, is smaller than that of the anions, $Cl^-$ ions. The total membrane potential difference, $\Delta\phi$, which is the summation of the two potential differences, increases slightly at the initial stage and decreases gradually with time. Although $\Delta\phi$ has slightly positive values, the electrochemical potential difference, $\Delta\mu_i$, for the three cations has negative values throughout the entire time period as shown in part c of Figure 2 because the initial

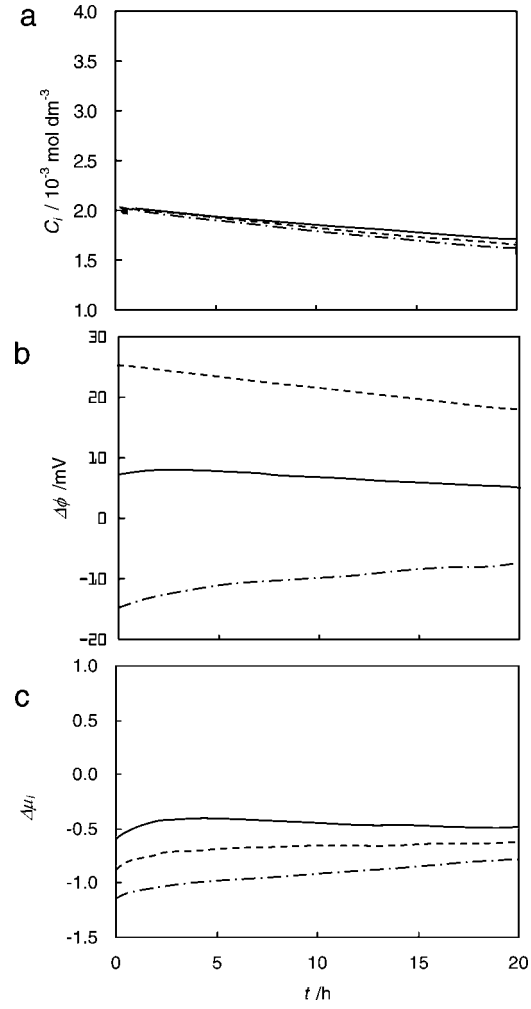


**Figure 2.** Simulations of the evolution of ionic transport in the system shown in Figure 1 when the charge density is 0.035 mol $dm^{-3}$. (a) The concentration of the cations in chamber I: solid curve, $La^{3+}$ ions; dashed curve, $Ca^{2+}$ ions; dash-dotted curve, $Li^+$ ions. (b) The electric potential differences: solid curve, the total membrane potential difference between the chambers; dashed curve, the summation of Donnan potential differences at the two membrane/solution interfaces; dashed-dotted curve, the diffusion potential difference across the membrane. (c) The electrochemical potential difference of the cations between the two chambers: solid curve, $La^{3+}$ ions; dashed curve, $Ca^{2+}$ ions; dash-dotted curve, $Li^+$ ions. The electric potential differences and electrochemical potential differences have positive values if the potentials in chamber II are higher than those in chamber I.

concentrations of the cations in chamber I are higher than those in chamber II. Therefore, type A transport occurs under these conditions.

Figure 3 shows the simulations when the charge density is 0.06 mol $dm^{-3}$. Part a of Figure 3 shows that the concentration of $La^{3+}$ ions in chamber I (the high-concentration side) increases with time at the initial stage, while the concentrations of the other cations decrease. This means that $La^{3+}$ ions are transported against their own concentration gradient. The transport situation in which the uphill transport of just the trivalent ions occurs is defined as type B. Part b of Figure 3 shows that $\Delta\phi$ under these conditions is higher than that when $C_x = 0.035$ mol $dm^{-3}$, as shown in Figure 2. The higher value of $\Delta\phi$ gives $\Delta\mu_i$ of $La^{3+}$ ions positive values during the initial stage, even though the initial concentration of $La^{3+}$ ions in chamber I is higher than that in chamber II. Therefore, $La^{3+}$ ions are transported against their own concentration gradient but along their own electrochemical potential gradient between the chambers. The $\Delta\mu_i$

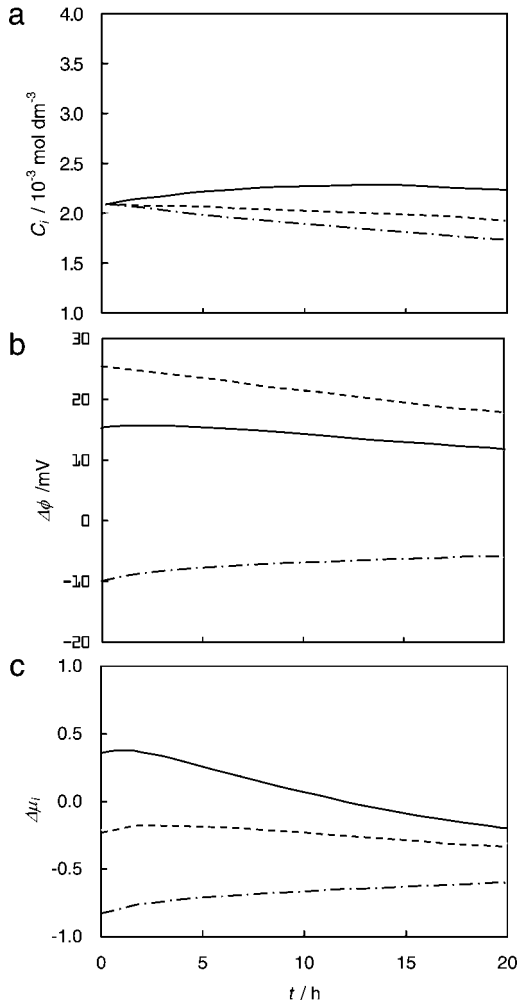


**Figure 3.** Simulations of the evolution of ionic transport in the dialysis system when the charge density is 0.06 mol dm$^{-3}$. Parts a−c are the same as in Figure 2.

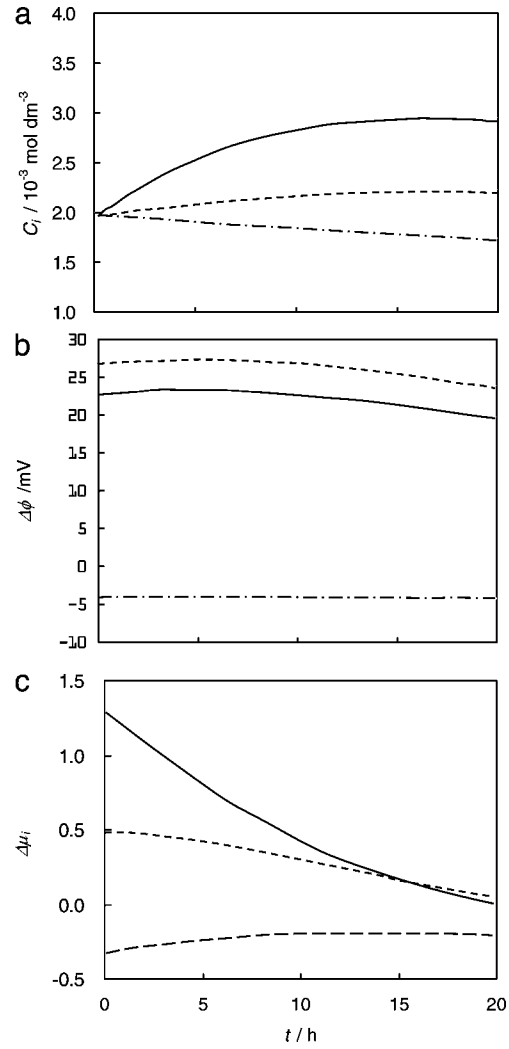


**Figure 4.** Simulations of the evolution of ionic transport in the dialysis system when the charge density is 0.10 mol dm$^{-3}$. Parts a−c are the same as in Figure 2.

value of $La^{3+}$ ions is found to decrease with time and has negative values when $t > 15$ h because the concentration difference of $La^{3+}$ ions between the two chambers increases with time while $\Delta\phi$ decreases. Hence, the transport mode of $La^{3+}$ ions switches from uphill to downhill when $t > 15$ h.

Part a of Figure 3 also shows that the initial slope of the time−concentration curve of the trivalent ions has a positive value while that of the bivalent cations is almost equal to zero. This means permselectivity between the trivalent ions and the bivalent cations has an almost infinite value and only the trivalent ions are concentrated in the high-concentration side at the initial stage.

The valence-selective transport of the cations occurs because of the following two factors: (1) the Donnan equilibrium and (2) the diffusion potential difference. Equation 2 indicates that the concentration ratio of the *i*th ion in the gel membrane and in solution is equal to the ionic valence power of the Donnan equilibrium constant *K*. Equations 1 and 2 give the value of *K* at the low-concentration side (chamber II) to be higher than that at the high-concentration side (chamber I). For these reasons, the concentration of the trivalent cations at the membrane/solution interface in chamber II is larger than that in chamber I under appropriate conditions. As a result, the concentration gradient of the trivalent cations in the membranes is in the opposite direction to that between the two chambers. The direction of the concentration gradient in the membrane depends on both the membrane charge density and the valence of the cations. The higher valence cations have, at the lower membrane charge density, the concentration gradients that occur in the opposite direction.

The other reason why valence-selective uphill transport occurs is because of the diffusion potential difference generated by the diffusion of the driving electrolyte. As shown in eq 16, the electrical potential energy of the *i*th ion is proportional to the valence of the ion. Hence, the higher valence ions have a stronger electrical force due to the diffusion potential they receive.

Figure 4 shows the simulations when the charge density is 0.10 mol dm$^{-3}$. Part a of Figure 4 shows that the concentrations of both $La^{3+}$ and $Ca^{2+}$ ions in chamber I increase with time at the initial stage while the concentration of $Li^+$ ions decreases. This means that uphill transport of the tri- and bivalent cations occurs. This transport situation is defined as type *C*. The value of $\Delta\phi$ under the conditions is higher than that when $C_x = 0.06$ mol dm$^{-3}$. The higher value of $\Delta\phi$ gives both $La^{3+}$ and $Ca^{2+}$ ions positive $\Delta\mu_i$ values at the initial stage, even though their concentrations in chamber I are higher than those in chamber II.

Figure 5 shows the simulations when the charge density is 0.25 mol dm$^{-3}$. Part a of Figure 5 shows that the concentrations of the three cations increase with time at the initial stage. This

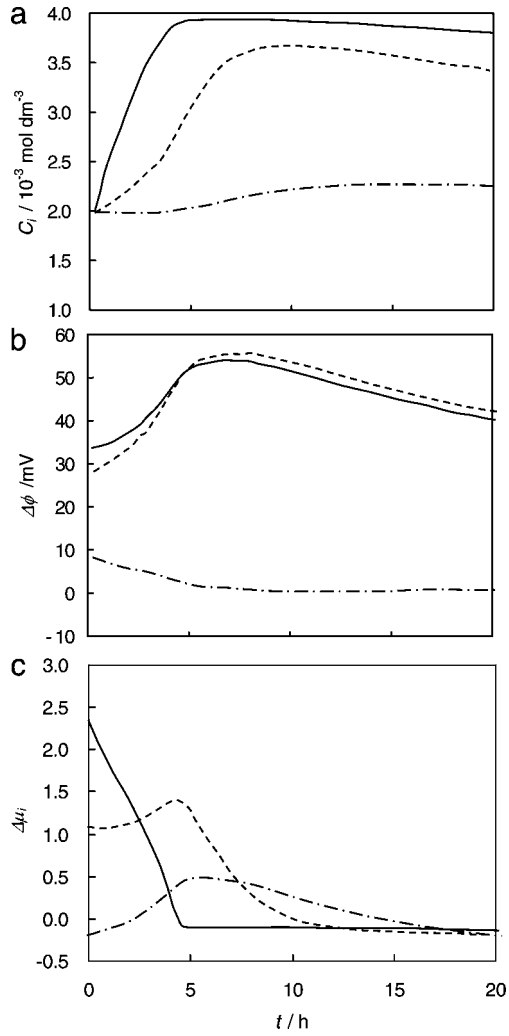


**Figure 5.** Simulations of the evolution of ionic transport of the dialysis system when the charge density is 0.25 mol dm$^{-3}$. Parts a−c are the same as in Figure 2.

means that uphill transport of the three cations occurs. This transport situation is defined as type *D*. Part b of Figure 5 shows that the initial value of $\Delta\phi$ under these conditions is higher than that when $C_x = 0.1$ mol dm$^{-3}$. Here, the $\Delta\phi_{don}$ value increases and has a maximum at 7 h, but then it decreases with time. This is because the uphill transport of $La^{3+}$ ions at the initial stage causes a decrease in their concentration in chamber II; hence, the composition in the concentration of the trivalent cations in chamber II solution containing tri-, bi-, and univalent ions decreases. The decrease in the composition of the trivalent ions in the solution causes an increase in the Donnan potential difference at the negatively charged membrane/solution interface, $\Delta\phi_{don}^{II}$ in eq 2.[44] Therefore, $\Delta\phi_{don}$ and $\Delta\phi$ increase with time at the initial stage and decrease with time after 7 h because the concentration difference of the driving electrolyte between the two chambers decreases with time, while the composition of the trivalent ions maintains a low value. The $\Delta\mu_i$ value of $La^{3+}$ ions decreases steeply with time because their concentration difference between the two chambers increases. Therefore, the flux of the cations which is proportional to the slope of the time−concentration curve decreases with time. When the uphill transport of the cations is suppressed by the increase in concentration difference between the two chambers, the uphill transport of both $Ca^{2+}$ and $Li^+$ ions is enhanced to compensate for the diffusion of the driving ions.

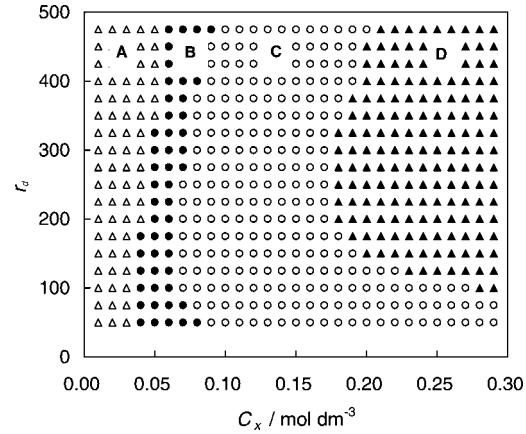


**Figure 6.** Simulations of the transport types in the dialysis system as functions of the charge density, $C_x$, and the concentration ratio of the driving electrolyte between the two chambers, $r_d$. Open triangles, type A; solid circles, type B; open circles, type C; solid triangles, type D, where $C_0$ is $5.0 \times 10^{-4}$ mol dm$^{-3}$ and $r_u$ is 4.

When the permeation time is about 5 h, the concentration of $La^{3+}$ ions in chamber I is almost equal to $4 \times 10^{-3}$ mol dm$^{-3}$. This means that their concentration in chamber II is close to zero because almost all of the $La^{3+}$ ions in chamber II are transported to chamber I against their own concentration gradients. The high concentration ratio of the cations between the two chambers and the decrease in the concentration gradient of the driving electrolyte gives negative $\Delta\mu_i$ values for $La^{3+}$ ions at $t \approx 5$ h. Hence, the transport mode of the cations changes from uphill to downhill. Therefore, the concentration ratio of $La^{3+}$ ions between the two chambers has a maximum value at 5 h. Here, $MCR_k$ is defined as the maximum concentration ratio for $k$ species cations between the two chambers. When the charge density is much higher than the ionic concentrations in the two chambers, the diffusion of the driving cations is perfectly coupled with the transport of the transport-controlled cations. In other words, the uphill transport efficiency, $\sigma$, which is defined by the following equation, is 100%:

$$\sigma \equiv \frac{z_c J_c(t) + z_a J_a(t)}{z_c J_c(t)} \times 100 \tag{22}$$

where $z_c$ and $J_c(t)$ are the valence and flux at time $t$ of the driving cations and $z_a$ and $J_a(t)$ are those of the driving anions, respectively. In a dialysis system where the concentration ratio of the driving cations between chambers I and II is kept constant (stationary state), the maximum concentration ratio of the uphill-transported $k$ species ions is defined as

$$MCR_k \equiv \left(\frac{C_k^{II}}{C_k^{I}}\right)_{stat} \tag{23}$$

where $C_k^{II}/C_k^{I}$ is the maximum concentration ratio of uphill-transported $k$ species ions between the two chambers. The system maintains $MCR_k$ as a constant value during the permeation time. Under the conditions (1) in the stationary state and (2) $\sigma = 100\%$, the value of $MCR_k$ can be estimated in terms of the theory by Schwahn and Woermann[31] as the simple mathematical expression:

$$MCR_k = \left(\frac{C_k^{II}}{C_k^{I}}\right)_{stat} = \left(\frac{C_c^{II}}{C_c^{I}}\right)_{stat}^{z_k} \tag{24}$$

where $C_c^{II}/C_c^{I}$ is the concentration ratio of the driving cations between the two chambers.

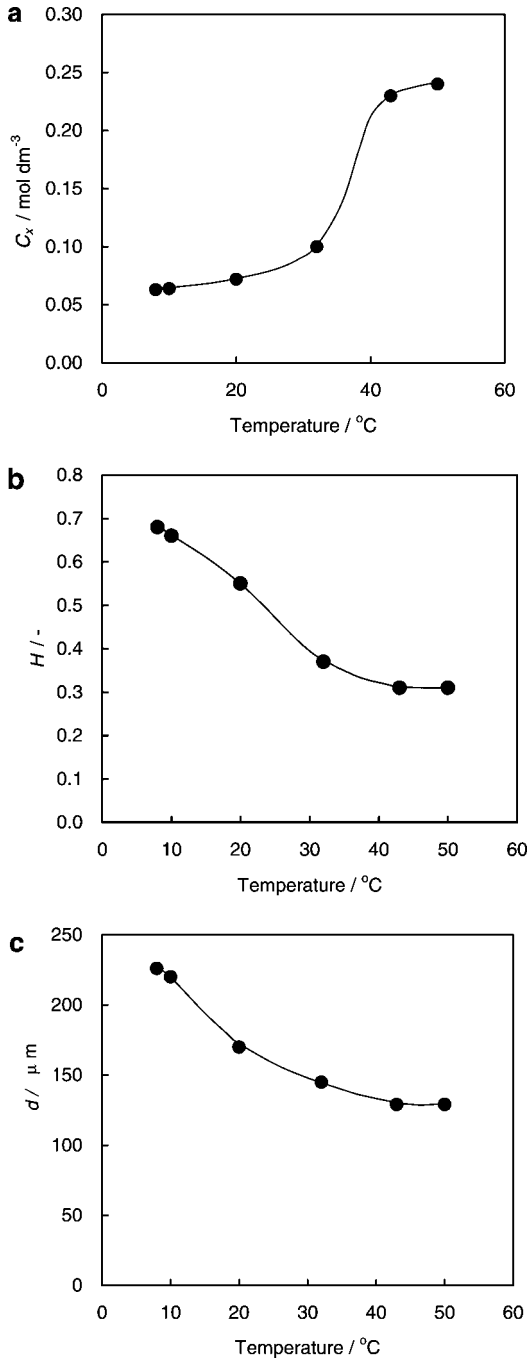


**Figure 7.** Temperature response of the gel membrane. (a) Charge density, (b) water content, and (c) thickness.

On the other hand, a general dialysis system where the uphill transport of $k$ species ions occurs in a nonstationary state has a maximum concentration ratio, $\mathrm{MCR}_k(t_k^m)$:

$$\mathrm{MCR}_k(t_k^m) \equiv \frac{C_k^{\mathrm{II}}(t_k^m)}{C_k^{\mathrm{I}}(t_k^m)} \tag{25}$$

at a certain permeation time, $t_k^m$, as shown in part a of Figures 3–5. Here, $MCR_k(t_k^m)$ decreases with decreasing charge density because when the charge density is lower than the ionic concentrations in the two chambers, $\sigma$ is not 100%. Here, $\sigma$ decreases with decreasing charge density due to the diffusion of the anions of the driving electrolyte. Both $\mathrm{MCR}_k(t_k^m)$ and $t_k^m$ also depend on the valence of the transport-controlled cations and on the composition and concentration of ions in the two chambers.

To evaluate the valence selectivity in uphill transport in the system, when the transport types B, C, and D occur, the valence-selective coefficient between the $p$ and $q$ species cations at time $t$, $\alpha_q^p(t)$, is defined as

$$\alpha_q^p(t) \equiv \frac{C_p^{\mathrm{I}}(t) - C_p^{\mathrm{I}}(0)}{C_q^{\mathrm{I}}(t) - C_q^{\mathrm{I}}(0)} \tag{26}$$

where $p$ denotes the uphill transported cations. The valence of the $p$ species cations is larger than that of the $q$ species cations. $C_p^{\mathrm{I}}(t)$ and $C_q^{\mathrm{I}}(t)$ are the concentrations of $p$ and $q$ species cations in chamber I at time $t$, respectively; $C_p^{\mathrm{I}}(0)$ and $C_q^{\mathrm{I}}(0)$ are the initial concentrations of these ions. When $\alpha_q^p(t) > 0$, uphill transport of both $p$ and $q$ species cations occurs. When $\alpha_q^p(t) < 0$, uphill transport of just the $p$ species cations occurs. We define $t_{pq}^{\alpha}$ as the time when $\alpha_q^p(t)$ has a maximum value. In this case, $t_{pq}^{\alpha}$ is not always equal to $t_k^m$. For example, when the charge density is 0.25 mol dm$^{-3}$, part a of Figure 5 shows that the trivalent cations have a $\mathrm{MCR}_k(t_k^m)$ value when $t_k^m = 5$ h. At the time, the concentrations of the trivalent and bivalent cations in chamber I are $3.9 \times 10^{-3}$ mol dm$^{-3}$ and $3.1 \times 10^{-3}$ mol dm$^{-3}$, respectively; hence, $\alpha_{\mathrm{Ca}}^{\mathrm{La}}(5)$ is 1.7. The corresponding concentrations at $t = 3$ h are $3.5 \times 10^{-3}$ mol dm$^{-3}$ and $2.3 \times 10^{-3}$ mol dm$^{-3}$, respectively; $\alpha_{\mathrm{Ca}}^{\mathrm{La}}(3)$ is 5.0. Hence, the valence selectivity in uphill transport has a maximum at $t = 3$ h. This is due to the flux of the trivalent cations being much higher than that of the other cations at the initial stage, and the difference in the flux between the trivalent cations and the other cations decreases with permeation time. Here, $\alpha_q^p(t)$ also depends on the composition and concentration of ions in the chambers, the valence and mobility of these ions, and the membrane charge density. The compositions and concentrations of ions in both chambers change with time. The system will have a higher $\alpha_q^p(t)$ value to control the charge density according to the changes in composition and concentrations of ions in the system. The optimal value of membrane charge density can be estimated using the simulations.

We simulated the ionic transport in the system under the approximation of a constant concentration gradient in the gel membrane, as shown in eq 4, or under the approximation of a constant electric field gradient in the membrane, as shown in eq 13. There is little difference between the simulations for the two approximations under these experimental conditions. Hence, the calculations in this study were performed using eq 4.

***B. Transport Types of Cations as Functions of the Charge Density and the Concentration Ratio of the Driving Electrolyte.*** Figure 6 shows the simulations of the transport types in the dialysis system as functions of the charge density and the concentration ratio of the driving electrolyte between the two chambers. The simulations show that type D transport does not occur when $r_{\mathrm{d}} < 100$. The simulations also indicate that the transport types in the system can be controlled by changing the charge density. For example, when, $r_{\mathrm{d}} = 300$, types A, B, C, and D transport occur in the range of the charge density as $C_x < 0.05$ mol dm$^{-3}$, 0.05 mol dm$^{-3}$ $< C_x <$ 0.07 mol dm$^{-3}$, 0.07 mol dm$^{-3}$ $< C_x <$ 0.18 mol dm$^{-3}$, and 0.18 mol dm$^{-3}$ $< C_x$, respectively. The simulations also indicate that the higher $r_{\mathrm{d}}$ the system has at the lower charge density, the uphill transport of ions with lower valence occurs. For example, type D transport occurs in lower charge density regions as $r_{\mathrm{d}}$ increases. Interestingly, when $r_{\mathrm{d}} > 300$, type D transport occurs in the higher charge density regions, because the increase in $r_{\mathrm{d}}$ corresponds

**TABLE 1: Characteristics of the T-Sensitive Anionic Gel Membrane at Various Temperatures**

| $T$ (°C) | $C_x$ (mol dm$^{-3}$) | $H$ | $d$ ($\mu$m) | $\omega_{Na}{}^a$ ($10^{-14}$ mol m$^2$ J$^{-1}$ s$^{-1}$) | $\omega_{Cl}{}^a$ ($10^{-14}$ mol m$^2$ J$^{-1}$ s$^{-1}$) | $\omega_{Li}{}^a$ ($10^{-14}$ mol m$^2$ J$^{-1}$ s$^{-1}$) | $\omega_{Ca}{}^a$ ($10^{-14}$ mol m$^2$ J$^{-1}$ s$^{-1}$) | $\omega_{La}{}^a$ ($10^{-14}$ mol m$^2$ J$^{-1}$ s$^{-1}$) |
|---|---|---|---|---|---|---|---|---|
| 10 | 0.064 | 0.66 | 220 | 4.8 | 6.8 | 2.0 | 1.2 | 0.79 |
| 32 | 0.10 | 0.37 | 145 | 0.39 | 0.55 | 0.16 | 0.094 | 0.064 |
| 50 | 0.24 | 0.31 | 130 | 0.32 | 0.45 | 0.13 | 0.077 | 0.052 |

[a] Calculated in terms of eq 19.

to an increase in the total ionic concentration in chamber I. Hence, the effect of the charge density on the ionic transport decreases with increasing ionic concentration. The simulation shows that the transport types in the system depend on the concentration and composition of ions in the two chambers and on the charge density. This means that an external-stimuli responsive ionic gel membrane whose charge density changes in response to external stimuli can dynamically control the valence-selective transport of ions in the dialysis system under situations in which the concentration and composition of ions in the system change during permeation experiments.

**Comparison of Simulations with Experiments.** To examine the prediction of the simulation experimentally, the permeation experiments in a dialysis system consisting of a temperature responsive anionic gel membrane and mixed NaCl, LiCl, $CaCl_2$, and $LaCl_3$ electrolyte solutions were carried out at various temperatures. Parts a−c of Figure 7 show the charge density, water content, and thickness of the gel membrane used in the permeation experiment as a function of temperature.

***A. Setup of the Permeation Conditions.*** The temperatures in the permeation experiments were chosen to control the transport types. The simulations shown in Figure 6 indicate that, at $r_d = 300$, the transport types B, C, and D occur when 0.05 mol dm$^{-3}$ < $C_x$ < 0.07 mol dm$^{-3}$, 0.07 mol dm$^{-3}$ < $C_x$ < 0.18 mol dm$^{-3}$, and 0.18 mol dm$^{-3}$ < $C_x$, respectively. Part a of Figure 7 indicates that the charge densities of the gel membrane at 10, 32, and 50 °C are 0.064, 0.10, and 0.24 mol dm$^{-3}$, respectively. Hence, the system using the gel membrane will show the transport types B, C, and D at 10, 32, and 50 °C, respectively. The water content of the gel at 10, 32, and 50 °C was obtained from part b of Figure 7 and the thickness of the gel from part c of Figure 7. The ionic mobilities in the gel membrane at these temperatures are estimated by substituting the values of the water content into eq 19. Higa et al.[45] also estimated the ionic mobility through a temperature-responsive nonionic gel membrane prepared from an in situ polymer of *N*-isopropylacrylamide and PVA. From these results, assuming that the value of $a$ in eq 19 for the T-responsive anionic gel membrane is independent of temperature and is the same as that of the T-responsive nonionic gel membrane, we set $a$ for the ions in the T-responsive anionic gel membrane as

$$a = 0.57 \text{ for } Na^+ \text{ ions}, \quad a = 0.30 \text{ for } Li^+ \text{ ions},$$
$$a = 0.23 \text{ for } Ca^{2+} \text{ ions}, \quad a = 0.20 \text{ for } La^{3+} \text{ ions},$$
$$a = 0.53 \text{ for } Cl^- \text{ ions} \quad (27)$$

The values of the charge density, water content, and thickness of the membrane and the ionic mobilities in the membrane are listed in Table 1. The permeation experiments using the membrane are compared with the simulations calculated by substituting the values into the equations in the Calculations section.

***B. Temperature Control of Valence Selective Uphill and Downhill Transport Modes of Ions.*** Part a of Figure 8 shows the time−concentration curves of $Li^+$, $Ca^{2+}$, and $La^{3+}$ ions at

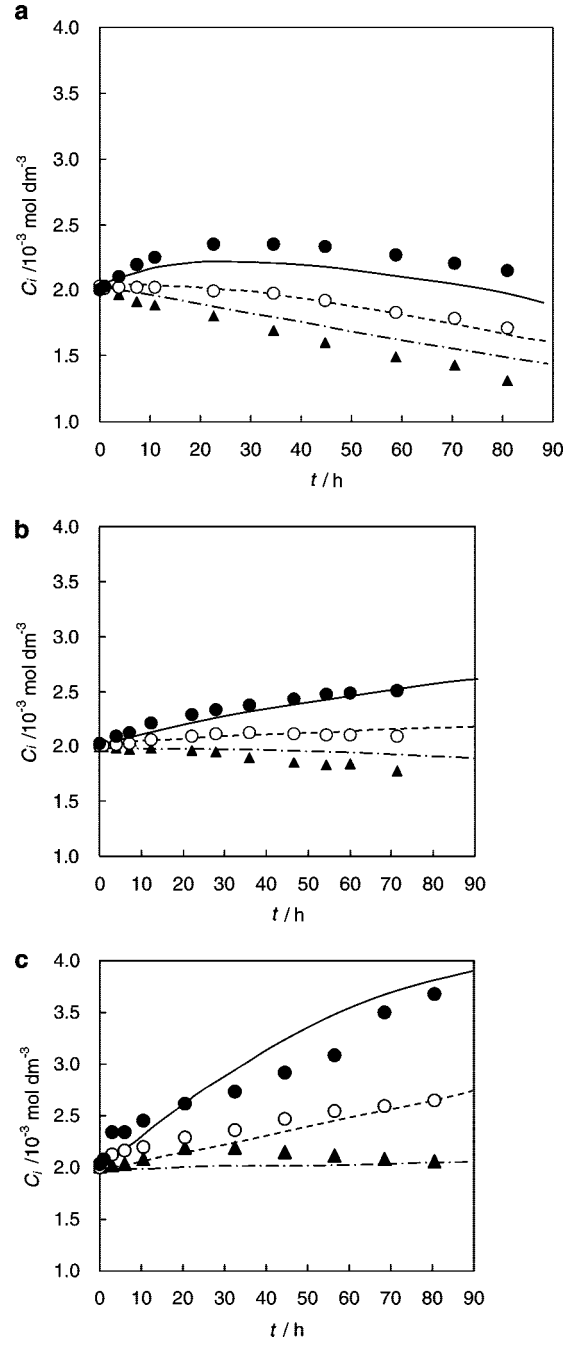


**Figure 8.** Experiments and simulations of the time−concentration curves of $La^{3+}$ ions, $Ca^{2+}$ ions, and $Li^+$ ions in chamber I (the high-concentration side) at (a) 10 °C, (b) 32 °C, and (c) 50 °C. Experiments: solid circles, $La^{3+}$ ions; open circles, $Ca^{2+}$ ions; solid triangles, $Li^+$ ions. Simulations: solid curve, $La^{3+}$ ions; dashed curve, $Ca^{2+}$ ions; dashed-dotted curve, $Li^+$ ions.

chamber I in the case that the temperature in the system maintains at 10 °C during the permeation experiment. The concentration of just $La^{3+}$ ions in the high-concentration side chamber increases with time while the concentration of $Li^+$ and

$Ca^{2+}$ ions decreases. This indicates that $La^{3+}$ ions are transported against their own concentration gradient between the two chambers. Hence, transport type B occurs under the conditions. Part b of Figure 8 shows the time evolution of the three cations at chamber I at 32 °C. The concentration of both $La^{3+}$ ions and $Ca^{2+}$ ions in the high-concentration side chamber increases with time while the concentration of $Li^{+}$ ions decreases. This indicates that the uphill transport of the two cations occurs. Hence, the transport type C occurs when the temperature is 32 °C. Part c of Figure 8 shows the time evolution of the three cations at chamber I at 50 °C. The concentrations of $La^{3+}$ ions, $Ca^{2+}$ ions, and $Li^{+}$ ions in the high-concentration side chamber increase with time. This indicates that the uphill transport of the three cations occurs. Hence, the transport type D occurs when the temperature is 50 °C.

The prediction of the simulation for the time−concentration profile in the system agrees almost quantitatively with the experimental data at all the temperatures. This means that the valence selectivity of all the cations in the proposed system will be predicted using the simulation method. The deviation between the simulations and the experiments probably comes from the following factors: (1) the water content shown in part b of Figure 7 measured by immersing the membrane into deionized water may have values different from that present during the permeation experiment because of the osmotic pressure difference caused by the high concentration of the driving electrolyte; (2) the ionic mobility in the membrane will be smaller than that obtained from eq 19 for the simulations. In other word, the assumptions in the simulations that the value of $a$ in the T-responsive anionic gel membrane is independent of temperature and is the same as that of the T-sensitive nonionic gel membranes will not be appropriate for the simulations in the experiment system. (3) The assumption that the standard chemical potentials in the membrane are equal to those in the solutions will be not appropriate for the simulations because changes in the hydrophilicity of the gel membrane with temperature results in changes in the standard chemical potentials of ions. The measurement of the mobility and standard chemical potential of ions in the T-responsive anionic gel is needed for reducing the deviation.

## Conclusion

Here, we have simulated the transport modes of ions in a dialysis system consisting of an ionic gel membrane and mixed solutions containing a driving electrolyte and electrolytes with uni-, bi-, and trivalent cations. The simulations show that the system has the four transport types in the transport modes of the cations: downhill and uphill in response to membrane charge density: (A) downhill transport of all the cations; (B) uphill transport of trivalent cations, downhill transport of the other cations; (C) uphill transport of bi- and trivalent ions, downhill transport of univalent ions; and (D) uphill transport of all the cations except for the driving cations. The simulations also indicate that the transport types in a dialysis system consisting of mixed electrolyte solutions and a temperature-responsive ionic gel membrane whose charge density changes in response to the temperature can be controlled by changing the temperature. The simulations agree nearly quantitatively with the experiments using a temperature-responsive anionic gel prepared from a modified PVA polymer containing 2 mol % of sulfonic acid groups and modified PVA prepared by in situ polymerization of *N*-isopropylacrylamide in a PVA solution.

In this study, the ionic transport in a batch type dialysis system was simulated. Our simulation method can be applied to a continuous dialysis system for estimating the optimum conditions for obtaining the highest valence selectivity in the uphill transport by controlling the charge density according to the compositions and concentrations of ions in the system.

**Acknowledgment.** This work was supported by a Grant-in-Aid for Scientific Research on Priority Areas (A) (No. 13022245), and a Grant-in-Aid for Scientific Research (C) (No. 13640581), from the Ministry of Education, Culture, Sports, Science, Technology, and also supported by the Salt Science Research Foundation (Nos. 0309, 0612, and 0709) and the Electric Technology Research Foundation of Chugoku (No. 89).

## References and Notes

(1) Tanaka, T. *Phys. Rev. Lett.* **1978**, *40*, 820.
(2) Tanaka, T.; Fillmore, D.; Sun, S.-T.; Nishio, I.; Swislow, G.; Shah, A. *Phys. Rev. Lett.* **1980**, *45*, 1636.
(3) Siegel, R. A.; Firestone, B. A. *Macromolecules* **1988**, *21*, 3254.
(4) Hirokawa, Y.; Tanaka, T. *J. Chem. Phys.* **1984**, *81*, 6379.
(5) Hoffman, A. S. *J. Controlled Release* **1987**, *6*, 297.
(6) Bae, Y. H.; Okano, T.; Hsu, R.; Kim, S. W. *Makromol. Chem., Rapid Commun.* **1987**, *8*, 481.
(7) Okano, T.; Bae, Y. H.; Jacobs, H.; Kim, S. W. *J. Controlled Release* **1990**, *11*, 255.
(8) Dong, L.-C.; Hoffman, A. S. *J. Controlled Release* **1991**, *15*, 141.
(9) Chen, G.; Hoffman, A. S. *Nature* **1995**, *373*, 49.
(10) Yoshida, R.; Uchida, K.; Kaneko, Y.; Sakai, K.; Kikuchi, A.; Sakurai, Y.; Okano, T. *Nature* **1995**, *374*, 240.
(11) Aoki, T.; Kawashima, M.; Katono, H.; Sanui, K.; Ogata, N.; Okano, T.; Sakurai, Y. *Macromolecules* **1994**, *27*, 947.
(12) Snowden, M. J.; Chowdhry, B. Z.; Vincent, B.; Morris, G. E. *J. Chem. Soc., Faraday Trans.* **1996**, *92*, 5013.
(13) Feil, H.; Bae, Y. H.; Feijen, J.; Kim, S. W. *J. Membrane Sci.* **1991**, *64*, 283.
(14) Tanaka, T.; Nishio, I.; Sun, S.-T.; Ueno-Nishio, S. *Science* **1982**, *218*, 467.
(15) Kwon, I. C.; Bae, Y. H.; Kim, S. W. *Nature* **1991**, *354*, 291.
(16) Osada, Y.; Okuzaki, H.; Hori, H. *Nature* **1992**, *355*, 242.
(17) Ishihara, K.; Hamada, N.; Kato, S.; Shinohara, I. *J. Polym. Sci., Polym. Chem.* **1984**, *22*, 881.
(18) Suzuki, A.; Tanaka, T. *Nature* **1990**, *346*, 345.
(19) Suzuki, A.; Ishii, T.; Maruyama, Y. *J. Appl. Phys.* **1996**, *80*, 131.
(20) Miyata, T.; Asami, N.; Uragami, T. *Nature* **1999**, *399*, 766.
(21) Kokufuta, E.; Zhang, Y.-Q.; Tanaka, T. *Nature* **1991**, *351*, 302.
(22) Miyata, T.; Jikihara, A.; Nakamae, K.; Hoffman, A. S. *Macromol. Chem. Phys.* **1996**, *197*, 1135.
(23) Kost, J.; Horbett, T. A.; Ratner, B. D.; Singh, M. *J. Biomed. Mater. Res.* **1985**, *19*, 1117.
(24) Kitano, S.; Koyama, Y.; Kataoka, K.; Okano, T.; Sakurai, Y. *J. Controlled Release* **1992**, *19*, 161.
(25) Kataoka, K.; Miyazaki, H.; Bunya, M.; Okano, T.; Sakurai, Y. *J. Am. Chem. Soc.* **1998**, *120*, 12694.
(26) Higa, M.; Yamakawa, T. *J. Phys. Chem. B* **2004**, *108*, 16703.
(27) Higa, M.; Yamakawa, T. *J. Phys. Chem. B* **2005**, *109*, 11373.
(28) Teorell, T. *Proc. Soc. Exp. Biol. Med.* **1935**, *33*, 282.
(29) Teorell, T. *Trans. Faraday Soc.* **1937**, *33*, 939.
(30) Teorell, T. *Prog. Biophys. Biophys. Chem.* **1953**, *3*, 305.
(31) Schwahn, P.; Woermann, D. *Ber. Bunsen-Ges. Phys. Chem.* **1986**, *90*, 773.
(32) Higa, M.; Kira, A. *J. Phys. Chem.* **1992**, *96*, 9518.
(33) Donnan, F. G. *Z. Phys. Chem.* **1934**, *A168*, 369.
(34) Goldman, D. E. *J. Gen. Physiol.* **1943**, *27*, 37.
(35) Henderson, P. *Z. Phys. Chem.* **1907**, *59*, 118.
(36) Osterhoudt, H. W. *J. Phys. Chem.* **1974**, *78*, 408.
(37) Muhr, A. H.; Blanshard, J. M. V. *Polymer* **1982**, *23*, 1012.
(38) Zhang, X.; Hirota, N.; Narita, T.; Gong, J. P.; Osada, Y. *J. Phys. Chem. B* **1999**, *103*, 6069.
(39) Mackie, J. S.; Meares, P. *Proc. R. Soc. London* **1955**, *232*, 498A
(40) Higa, M.; Koga, M.; Tanioka, A. *Sen'i Gakkaishi* **2000**, *56*, 290.
(41) *International Critical Tables*; McGraw-Hill: New York, 1949.
(42) Yamakawa, T.; Ishida, S.; Higa, M. *J. Membr. Sci.* **2005**, *250*, 61.
(43) Meyer, K. H.; Sievers, J.-F. *Helv. Chim. Acta* **1936**, *19*, 649.
(44) Higa, M.; Kira, A.; Tanioka, A.; Miyasaka, K. *J. Chem. Soc., Faraday Trans.* **1993**, *89*, 3433.
(45) Higa, M.; Nishimura, M.; Imura, T.; Miyamoto, C. Unpublished data.

JP711437M